Identification of Plitidepsin as Potent Inhibitor of SARS-CoV-2-Induced Cytopathic Effect After a Drug Repurposing Screen

Jordi Rodon[1], Jordana Muñoz-Basagoiti[2†], Daniel Perez-Zsolt[2†], Marc Noguera-Julian[2,3], Roger Paredes[2,4], Lourdes Mateu[4], Carles Quiñones[4], Carles Perez[5], Itziar Erkizia[2], Ignacio Blanco[6], Alfonso Valencia[5,7], Víctor Guallar[5,7], Jorge Carrillo[2], Julià Blanco[2,3,6], Joaquim Segalés[8,9], Bonaventura Clotet[2,3,6], Júlia Vergara-Alert[1]* and Nuria Izquierdo-Useros[2,6]*

[1]IRTA, Centre de Recerca en Sanitat Animal (CReSA, IRTA-UAB), Campus de la UAB, Bellaterra, Spain, [2]IrsiCaixa AIDS Research Institute, Badalona, Spain, [3]University of Vic–Central University of Catalonia (UVic-UCC), Vic, Spain, [4]Germans Trias i Pujol Hospital, Badalona, Spain, [5]Barcelona Supercomputing Center, Barcelona, Spain, [6]Germans Trias i Pujol Research Institute (IGTP), Can Ruti Campus, Badalona, Spain, [7]Catalan Institution for Research and Advanced Studies (ICREA), Barcelona, Spain, [8]UAB, CReSA (IRTA-UAB), Campus de la UAB, Bellaterra, Spain, [9]Departament de Sanitat i Anatomia Animals, Facultat de Veterinària, Bellaterra, Spain

There is an urgent need to identify therapeutics for the treatment of Coronavirus disease 2019 (COVID-19). Although different antivirals are given for the clinical management of SARS-CoV-2 infection, their efficacy is still under evaluation. Here, we have screened existing drugs approved for human use in a variety of diseases, to compare how they counteract SARS-CoV-2-induced cytopathic effect and viral replication in vitro. Among the potential 72 antivirals tested herein that were previously proposed to inhibit SARS-CoV-2 infection, only 18 % had an IC_{50} below 25 μM or 10^2 IU/ml. These included plitidepsin, novel cathepsin inhibitors, nelfinavir mesylate hydrate, interferon 2-alpha, interferon-gamma, fenofibrate, camostat along the well-known remdesivir and chloroquine derivatives. Plitidepsin was the only clinically approved drug displaying nanomolar efficacy. Four of these families, including novel cathepsin inhibitors, blocked viral entry in a cell—type specific manner. Since the most effective antivirals usually combine therapies that tackle the virus at different steps of infection, we also assessed several drug combinations. Although no particular synergy was found, inhibitory combinations did not reduce their antiviral activity. Thus, these combinations could decrease the potential emergence of resistant viruses. Antivirals prioritized herein identify novel compounds and their mode of action, while independently replicating the activity of a reduced proportion of drugs which are mostly approved for clinical use. Combinations of these drugs should be tested in animal models to inform the design of fast track clinical trials.

Keywords: SARS-CoV-2, antivirals, plitidepsin, synergy, viral entry

INTRODUCTION

A novel betacoronavirus, the severe acute respiratory syndrome coronavirus 2 (SARS-CoV-2), is causing a respiratory disease pandemic that began in Wuhan, China, in November 2019, and has now spread across the world (Chen et al., 2020b). To date, remdesivir is the only approved antiviral drug for the specific treatment of this coronavirus infectious disease 2019 or COVID-19 (Beigel et al., 2020; Grein et al., 2020). However, several drugs are being used in the frontline of clinical management of SARS-CoV-2-infected individuals in hospitals all around the world, to try to avoid the development of the COVID-19 associated pneumonia, which can be fatal. By the end of December 2020, almost 1.7 million people had died from COVID-19, and over 75 million cases have been reported (https://covid19.who.int).

Although different drug regimens are being applied to hospitalized patients, no clinical study has evidenced their efficacy yet. Under this scenario, initiatives launched by the World Health Organization (WHO), such as the SOLIDARITY study that has compared remdesivir, hydroxychloroquine, ritonavir/lopinavir and ritonavir/lopinavir plus ß-interferon regimes, have been of critical importance to prioritize the use of the most active compounds (WHO, 2020). Unfortunately, although remdesivir has proven efficacy in randomized controlled trials (Beigel et al., 2020; Grein et al., 2020), a recent update of the WHO clinical trial has failed to detect any effect on overall mortality, initiation of ventilation and duration of hospital stay with any of the antivirals tested (Pan, 2020). Thus, there is an urgent need to identify novel therapeutic approaches for individuals with COVID-19 developing severe disease and fatal outcomes.

In this report we present a prioritized list of effective compounds with proven antiviral efficacy *in vitro* to halt SARS-CoV-2 replication. Compounds were analyzed depending on their expected mechanism of action, to identify candidates tackling diverse steps of the viral life cycle. SARS-CoV-2 entry requires viral binding and spike protein activation via interaction with the cellular receptor ACE2 and the cellular protease TMPRSS2 at the plasma membrane (Hoffmann et al., 2020). Interference with either of these ligands has proven to decrease SARS-CoV-2 infectivity (Monteil et al. 2020; Hoffmann et al., 2020), and therefore, inhibitors targeting viral entry may prove valuable. In addition, SARS-CoV-2 enters into the cells via endocytosis and accumulates in endosomes where cellular cathepsins can also prime the spike protein and favor viral fusion upon cleavage (Simmons et al., 2005; Mingo et al., 2015; Hoffmann et al., 2020), providing additional targets for antiviral activity. Once SARS-CoV-2 fuses with cellular membranes, it triggers viral RNA release into the cytoplasm, where polyproteins are translated and cleaved by proteases (Song et al., 2019). This leads to the formation of an RNA replicase—transcriptase complex driving the production of several negative—stranded RNA via both replication and transcription (Song et al., 2019). Numerous negative-stranded RNAs transcribe into messenger RNA genomes, allowing for the translation of viral nucleoproteins, which assemble in viral capsids at the cytoplasm (Song et al., 2019). These capsids then bud into the lumen of endoplasmic reticulum (ER)-Golgi compartments, where viruses are finally released into the extracellular space by exocytosis. Potentially, any of these viral cycle steps could be targeted with antivirals, so we have thus searched for these compounds as well.

Finally, as the most effective antiviral treatments are usually based on combined therapies that tackle distinct steps of the viral life cycle, we also tested the active compounds in combination. These combinations may be critical to abrogate the potential emergence of resistant viruses and to increase antiviral activity, enhancing the chances to improve clinical outcome.

MATERIAL AND METHODS

Cell Cultures
Vero E6 cells (ATCC CRL-1586) were cultured in Dulbecco's modified Eagle medium (DMEM; Lonza) supplemented with 5% fetal calf serum (FCS; EuroClone), 100 U/ml penicillin, 100 µg/ml streptomycin, and 2 mM glutamine (all ThermoFisher Scientific). HEK-293T (ATCC repository) were maintained in DMEM with 10% fetal bovine serum, 100 IU/ml penicillin and 100 µg/ml streptomycin (all from Invitrogen). HEK-293T overexpressing the human ACE2 were kindly provided by Integral Molecular Company and maintained in DMEM (Invitrogen) with 10% fetal bovine serum, 100 IU/ml penicillin and 100 µg/ml streptomycin, and 1 µg/ml of puromycin (all from Invitrogen). TMPRSS2 human plasmid (Origene) was transfected using X-tremeGENE HP Transfection Reagent (Merck) on HEK-293T overexpressing the human ACE2 and maintained in the previously described media containing 1 mg/ml of geneticin (Invitrogen) to obtain TMPRSS2/ACE2 HEK-293T cells.

Virus isolation, Titration and Sequencing
SARS-CoV-2 was isolated from a nasopharyngeal swab collected from an 89-year-old male patient giving informed consent and treated with Betaferon and hydroxychloroquine for 2 days before sample collection. The swab was collected in 3 ml medium (Deltaswab VICUM) to reduce viscosity and stored at −80°C until use. Vero E6 cells were cultured on a cell culture flask (25 cm^2) at 1.5 x 10^6 cells overnight prior to inoculation with 1 ml of the processed sample, for 1 h at 37°C and 5% CO$_2$. Afterward, 4 ml of 2% FCS-supplemented DMEM were supplied and cells were incubated for 48 h. Supernatant was harvested, centrifuged at 200 × g for 10 min to remove cell debris and stored at −80°C. Cells were assessed daily for cytopathic effect and the supernatant was subjected to viral RNA extraction and specific RT-qPCR using the SARS-CoV-2 UpE, RdRp and N assays (Corman et al., 2020). The virus was propagated for two passages and a virus stock was prepared collecting the supernatant from Vero E6.

Viral RNA was extracted directly from the virus stock using the Indimag Pathogen kit (Indical Biosciences) and transcribed to cDNA using the PrimeScript™ RT reagent Kit (Takara) using oligo-dT and random hexamers, according to the manufacturer's protocol. DNA library preparation was performed using SWIFT amplicon SARS-CoV-2 panel (Swift Biosciences). Sequencing

ready libraries where then loaded onto Illumina MiSeq platform and a 300 bp paired-end sequencing kit. Sequence reads were quality filtered and adapter primer sequences were trimmed using trimmomatic. Amplification primer sequences were removed using cutadapt (Martin, 2011). Sequencing reads were then mapped against coronavirus reference (NC_045512.2) using bowtie2 tool (Langmead and Salzberg, 2012). Consensus genomic sequence was called from the resulting alignment at a $18 \times 1800 \times 879$ average coverage using samtools (Li et al., 2009). Genomic sequence was deposited at GISAID repository (http://gisaid.org) with accession ID EPI_ISL_510689.

Pseudovirus Production

HIV-1 reporter pseudoviruses expressing SARS-CoV-2 Spike protein and luciferase were generated using two plasmids. pNL4-3. Luc.R-E-was obtained from the NIH AIDS repository. SARS-CoV-2. SctΔ19 was generated (Geneart) from the full protein sequence of SARS-CoV-2 spike with a deletion of the last 19 amino acids in C-terminal, human-codon optimized and inserted into pcDNA3.4-TOPO (Ou et al., 2020b). Spike plasmid was transfected with X-tremeGENE HP Transfection Reagent (Merck) into HEK-293T cells, and 24 h post-transfection, cells were transfected with pNL4-3. Luc.R-.E-. Supernatants were harvested 48 h later, filtered with 0.45 μM (Millex Millipore) and stored at −80°C until use. Control pseudoviruses were obtained by replacing the spike plasmid by a VSV-G plasmid (kindly provided by Dr Andrea Cimarelli). The p24^{gag} content of all viruses was quantified using an ELISA (Perkin Elmer) and viruses were titrated in HEK-293T overexpressing the human ACE2.

Antivirals and Compounds

The complete list of compounds used for this study and vendors are shown in **Supplementary Tables S1–S5**. Drugs were used at concentrations ranging from 100 μM to 0.0512 nM at 5-fold serial dilutions. NPOs were used at concentrations ranging from 10 μM to 0.00512 nM at 5-fold serial dilutions. Plitidepsin was also assayed at concentrations ranging from 10 μM to 0.5 nM at 3-fold dilutions. Interferons were assayed at concentrations ranging from 10^4 to 0.0005 IU/ml at 5-fold serial dilutions. When two drugs were combined, each one was added at a 1:1 molar ratio at concentrations ranging from 100 μM to 0.0512 nM at 5-fold serial dilutions. In combination with other drugs, plitidepsin was also assayed at concentrations ranging from 10 μM to 0.5 nM at 3-fold dilutions.

Antiviral Activity

Increasing concentrations of antiviral compounds were added to Vero E6 cells and immediately after, we added $10^{1.8}$ TCID50/mL of SARS-CoV-2, a concentration that achieves a 50% of cytopathic effect (20 TCID$_{50}$ per well to 30,000 cells in 200 μl). Untreated non-infected cells and untreated virus-infected cells were used as negative and positive controls of infection, respectively. To detect any drug-associated cytotoxic effect, Vero E6 cells were equally cultured in the presence of increasing drug concentrations, but in the absence of virus. Cytopathic or cytotoxic effects of the virus or drugs were measured 3 days after infection, using the CellTiter-Glo luminescent cell viability assay (Promega). Luminescence was measured in a Fluoroskan Ascent FL luminometer (ThermoFisher Scientific).

## IC$_{50}$ Calculation and Statistical Analysis

Response curves of compounds or their mixes were adjusted to a non-linear fit regression model, calculated with a four-parameter logistic curve with variable slope. Cells not exposed to the virus were used as negative controls of infection, and were set as 100% of viability to normalize data and calculate the percentage of cytopathic effect. Statistical differences from 100% were assessed with a one sample t test. All analyses and figures were generated with the GraphPad Prism v8.0b Software.

In Silico Drug Modeling

We performed Glide docking on SARS-CoV-2 3CL Main protease using the DrugBank database (https://go.drugbank.com), with a total of 6837 molecules containing FDA approved drugs, reported phased I/II/III drugs and experimental molecules (i.e. drugs that are at the preclinical or animal testing stage) (Gupta and Zhou, 2020). For this, two different receptors were prepared, the 6LU7 pdb structure, after removing the covalently bound inhibitor, and a combination of two crystals from the Diamond collection (https://www.diamond.ac.uk/covid-19). This combination intended to open a bit more the active site by rotating Gln189 and exposing it more to the solvent, after visual inspection of the different fragment crystals. Receptors were prepared with the Schrodinger's protein wizard assigning protonation states at pH 7 using the interactive optimizer. Also, after inspection of the recent crystal structures, Glide SP docking was performed with two different (ligand) hydrogen bond constraints: Glu16 and His163 (this last residue with epsilon protonation); we enforced single constraints and also attempted the combination of both. The best 11 molecules, based on Glides's docking score, were selected for experimental validation. Notice, however, that top docking scores, did not exceed −9, indicating poor potential binding, in agreement with other non-productive repurposing efforts reported on SARS-CoV-2 main protease, including sophisticated *in silico* studies (Gupta and Zhou, 2020).

Pseudovirus Assay

HEK-293T overexpressing the human ACE2 and TMPRSS2 were used to test antivirals at the concentrations found to be effective for SARS-CoV-2 without toxicity, which were the following: 5 μM for niclosamide; 10 μM for chloroquine, chlorpromazine, ciclesonide, MDL 28170 and fenofibrate; 20 μM for hydroxychloroquine, CA-074-Me and arbidol HCl; 25 μM for E-64d; 50 μM for Baricitinib; 100 μM for Amantadine, NB-DNJ, 3' sialyl-lactose Na salt, tofacitinib, and Camostat mesylate; 1000 μM for methyl-β-cyclodextrin, and 12,5 mg/ml for AAT. A constant pseudoviral titer was used to pulse cells in the presence of the drugs. At 48 h post-inoculation, cells were lysed with the Glo Luciferase system (Promega). Luminescence was measured with an EnSight Multimode Plate Reader (Perkin Elmer).
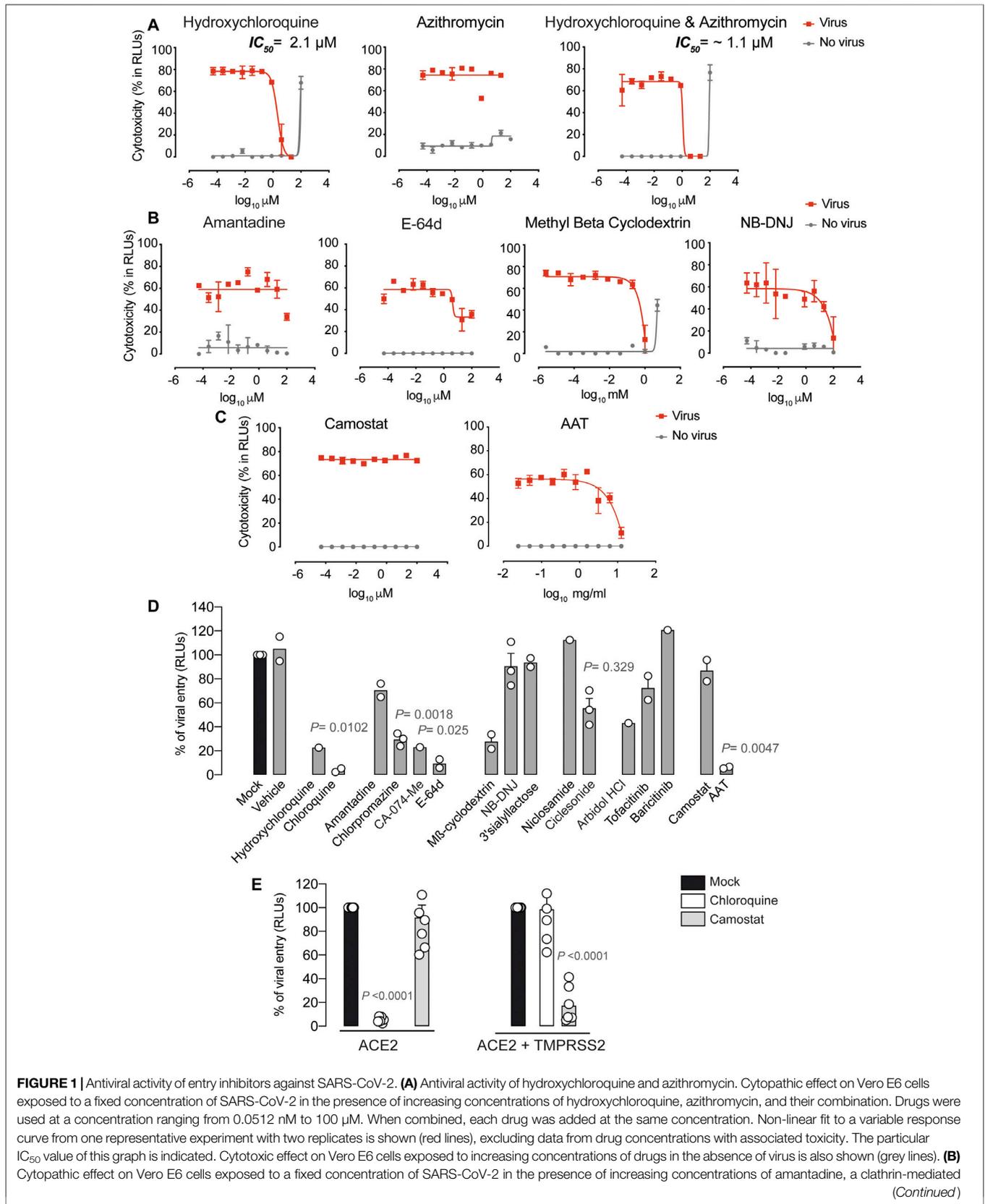
FIGURE 1 | Antiviral activity of entry inhibitors against SARS-CoV-2. **(A)** Antiviral activity of hydroxychloroquine and azithromycin. Cytopathic effect on Vero E6 cells exposed to a fixed concentration of SARS-CoV-2 in the presence of increasing concentrations of hydroxychloroquine, azithromycin, and their combination. Drugs were used at a concentration ranging from 0.0512 nM to 100 μM. When combined, each drug was added at the same concentration. Non-linear fit to a variable response curve from one representative experiment with two replicates is shown (red lines), excluding data from drug concentrations with associated toxicity. The particular IC$_{50}$ value of this graph is indicated. Cytotoxic effect on Vero E6 cells exposed to increasing concentrations of drugs in the absence of virus is also shown (grey lines). **(B)** Cytopathic effect on Vero E6 cells exposed to a fixed concentration of SARS-CoV-2 in the presence of increasing concentrations of amantadine, a clathrin-mediated
(Continued)

FIGURE 1 | endocytosis inhibitor, E-64d, a pan-cathepsin inhibitor acting downstream once viruses are internalized in endosomes, NB-DNJ, an inhibitor of ganglioside biosynthesis and methyl-β-cyclodextrin, a cholesterol-depleting agent. All drugs were used at a concentration ranging from 0.0512 nM to 100 μM aside from methyl-β-cyclodextrin, which was used 10 times more concentrated. Non-linear fit to a variable response curve from one experiment with two replicates is shown (red lines). Cytotoxic effect on Vero E6 cells exposed to increasing concentrations of drugs in the absence of virus is also shown (grey lines). **(C)** Cytopathic effect on Vero E6 cells exposed to a fixed concentration of SARS-CoV-2 in the presence of increasing concentrations of camostat, a TMPRSS2 inhibitor, and ATT, an alpha-1 antyitrypsin, a broad cellular protease inhibitor, as described in **(A)**. **(D)** Effect of entry inhibitors on luciferase expression of reporter lentiviruses pseudotyped with SARS-CoV-2 Spike in ACE2 expressing HEK-293T cells. Values are normalized to luciferase expression by mock-treated cells set at 100%. Mean and s.e.m. from two experiments with one to three replicates. Cells were exposed to fixed amounts of SARS-CoV-2 Spike lentiviruses in the presence of a non-toxic constant concentration of the drugs tested on Vero E6. Significant statistical deviations from 100% were assessed with a one sample *t* test. **(E)** Comparison of entry inhibitors blocking viral endocytosis, such as chloroquine, with inhibitors blocking serine protease TMPRSS2 expressed on the cellular membrane, such as camostat, on different cell lines. ACE2 expressing HEK-293T cells transfected or not with TMPRSS2 were exposed to SARS-CoV-2 Spike lentiviruses as described in **(B)**. Values are normalized to luciferase expression by mock-treated cells set at 100%. Mean and s.e.m. from at least two representative experiments with two replicates. Statistical deviations from 100% were assessed with a one sample *t* test.

SARS-CoV-2 Detection in the Supernatant of Infected Cells

Viral accumulation in the supernatant of Vero E6 cells infected as described previously in the presence of increasing concentrations of the indicated antiviral compounds was measured at day 3 post-infection. The amount of SARS-CoV-2 nucleoprotein released to the supernatant was measured with an ELISA (SinoBiologicals), according to the manufacturer's protocol. This ELISA contains a buffer to lyse viral membranes and release nucleoprotein content.

RESULTS

We have tested the antiviral activity of different clinically available compounds and their combinations by assessing their ability to inhibit viral induced cytopathic effect *in vitro*. Our strategy was circumscribed mostly to compounds approved for clinical use, since they are ideal candidates for entering into fast track clinical trials. Drug selection criteria first focused on compounds already being tested in clinical trials, along with well-known human immunodeficiency virus-1 (HIV-1) and hepatitis C virus (HCV) inhibitors, as well as other compounds suggested to have potential activity against SARS-CoV-2 in molecular docking analysis or *in vitro* assays (Chen et al., 2020a; Dittmar et al., 2020; Ianevski et al., 2020; Riva et al., 2020; Weston et al., 2020).

We first assessed the activity of 16 compounds with hypothetical capacity to inhibit viral entry, and then we focused on 22 drugs thought to block viral replication upon SARS-CoV-2 fusion. Molecular docking studies provided an additional 11 candidates, which were predicted to inhibit the SARS-CoV-2 main protease. Finally, 23 compounds with unknown mechanism of action were also assessed. By these means, we have compared 72 drugs and 28 of their combinations for their capacity to counteract SARS-CoV-2-induced cytopathic effect *in vitro*.

Antiviral Activity of Compounds that Potentially Inhibit Viral Entry

We first tested compounds that could have an effect before viral entry by impairing virus-cell fusion (**Supplementary Table S1**). We confirmed the inhibitory effect of hydroxychloroquine against SARS-CoV-2-induced cellular cytotoxicity on Vero E6 cells (Liu et al., 2020). As shown in **Figure 1A**, this drug was able to inhibit viral-induced cytopathic effects at concentrations where no cytotoxic effects of the drug were observed, as previously reported (Liu et al., 2020; Wang et al., 2020). Since hydroxychloroquine was first administered in combination with the antibiotic azithromycin (Gautret et al., 2020), which induces antiviral responses in bronchial epithelial cells (Gielen et al., 2010), we tested this antibiotic alone and in combination (**Figure 1A**), but found a similar activity to that of the chloroquine derivative alone (**Figure 1A**). Indeed, this was also the case when we tested hydroxychloroquine in combination with different HIV-1 protease inhibitors and other relevant compounds currently being tested in clinical trials (**Supplementary Table S2**).

Additional Food and Drug Administration (FDA)-approved compounds previously used to abrogate viral entry via clathrin-mediated endocytosis such as amantadine or chlorpromazine were also tested in this SARS-CoV-2-induced cytotoxicity assay (**Supplementary Table S2**). Yet, we did not find any prominent effect of these agents; only a partial inhibition at 100 μM for amantadine (**Figure 1B**). The broad cathepsin B/L inhibitor E64-d also showed partial inhibitory activity (**Figure 1B**). E64-d exerts activity against viruses cleaved by cellular cathepsins upon endosomal internalization, as previously described using pseudotyped SARS-CoV-2 (Hoffmann et al., 2020). While these results could not be confirmed using the specific cathepsin B inhibitor CA-074-Me due to drug-associated toxicity (**Supplementary Table S1**), none of these cathepsin inhibitors is approved for clinical use. It has also been suggested that hydroxychloroquine could block SARS-CoV-2 spike interaction with GM1 gangliosides (Fantini et al., 2020). GM1 gangliosides are enriched in cholesterol domains of the plasma membrane and have been previously shown to bind to SARS-CoV spike protein (Lu et al., 2008). This mode of viral interaction is aligned with the capacity of methyl-beta cyclodextrin, which depletes cholesterol from the plasma membrane to abrogate SARS-CoV-2 induced cytopathic effect (**Figure 1B**), as previously reported for SARS-CoV (Lu et al., 2008). Removal of cholesterol redirected ACE2 receptor to other domains, but did not alter the expression of the viral receptor (Lu et al., 2008). Moreover, NB-DNJ, an inhibitor of ganglioside biosynthesis pathway, also decreased SARS-CoV-2 cytopathic

effect (**Figure 1B**). These results highlight the possible role of gangliosides in viral binding, although in soluble competition the polar head group of GM3 ganglioside (3' Sialyllactose) was not able to reduce viral-induced cytopathic effect (**Supplementary Table S1**). Of note, previously reported antiviral agents such as the autophagy BECN1-stabilizing compounds niclosamide or ciclesonide (Gassen et al., 2020), (Jeon et al., 2020), the membrane lipid intercalating compound arbidol (Haviernik et al., 2018) and the two JAK inhibitors baricitinib and tofacitinib (Richardson et al., 2020; Stebbing et al., 2020) failed to protected Vero E6 cells from SARS-CoV-2 induced cytopathic effect (**Supplementary Table S1**). We next tested camostat, a serine protease inhibitor with capacity to abrogate SARS-CoV-2 Spike priming on the plasma membrane of human pulmonary cells and avoid viral fusion (Hoffmann et al., 2020). Camostat showed no antiviral effect on Vero E6 cells (**Figure 1C**), what indicates that the alternative viral endocytic route is the most prominent entry route in this renal cell type. A broader cellular protease inhibitor such as alpha-1 antitrypsin (AAT), used to treat severe AAT human deficiency and currently under clinical study for COVID-19 due to its anti-inflammatory potential, has already shown capacity to limit SARS-CoV-2 entry in cells expressing TMPRSS2 (Münch, 2020; Oguntuyo et al., 2020). When we tested AAT antiviral efficacy on Vero E6, AAT exerted an effect but required high concentrations that will most likely rely on the activity of these proteases in the endosomal route (**Figure 1C**).

To confirm that identified compounds listed in **Supplementary Table S1** specifically inhibit the viral entry step, we employed a luciferase-based assay using pseudotyped lentivirus expressing the spike protein of SARS-CoV-2, which allows to detect viral fusion on HEK-293 T cells transfected with ACE2. As a control, we used lentiviruses pseudotyped with a VSV glycoprotein, where no entry inhibition above 20 % was detected for any of the drugs tested (data not shown). In sharp contrast, SARS-CoV-2 pseudoviruses were effectively blocked by most of the drugs previously tested on Vero E6 with wild-type virus (**Figure 1D**). The main differences were observed with CA-074-Me, ciclesonide and arbidol. These compounds showed a partial blocking effect on ACE2 HEK-293T cells that was not obvious when using replication competent SARS-CoV-2 on Vero E6 (**Supplementary Figure S1**). In addition, NB-DNJ failed to block viral entry (**Figure 1D**). Overall, using alternative SARS-CoV-2 viral systems, we could identify chloroquine derivatives, cathepsin inhibitors and cholesterol depleting agents as the most promising candidates to block SARS-CoV-2 endocytosis in Vero E6 and HEK-293T cells transfected with ACE2. However, chloroquine derivatives were the only ones that displayed an IC_{50} below 25 µM (**Table 1**), and were also active abrogating pseudoviral entry into HEK-293 T cells expressing ACE2 (**Figure 1E**). Although camostat failed to inhibit viral fusion on ACE2 HEK-293T cells (**Figure 1E**), its activity was rescued when these cells were transfected with TMPRSS2. The opposite effect was observed for chloroquine, which reduced its inhibitory activity on TMPRSS2 transfected cells (**Figure 1E**). Our results

highlight that alternative routes govern SARS-CoV-2 viral entry and these pathways vary depending on the cellular target. Thus, effective treatments may need to block both plasma membrane fusion and endosomal routes to fully achieve viral suppression.

Antiviral activity of Compounds that Potentially Inhibit Post-entry Steps

In our search for antivirals inhibiting post-viral entry steps, we first focused on remdesivir, which has *in vitro* activity against SARS-CoV-2 after viral entry (Wang et al., 2020) and has already been approved for the treatment of COVID-19 by the FDA and the European Medicines Agency (EMA). We further confirmed the *in vitro* capacity of remdesivir to inhibit SARS-CoV-2-induced cytopathic effect on Vero E6 (**Figure 2A**). The IC_{50} value of this drug in repeated experiments was always below 10 µM (**Supplementary Table S2**). In combination with increasing concentrations of hydroxychloroquine, however, remdesivir did not significantly modified its own antiviral effect (**Figure 2B**). This was also the case for other antivirals tested in combination (**Supplementary Table S3**). Of note, other RNA polymerase inhibitors such as galdesivir, which was proposed to tightly bind to SARS-CoV-2 RNA-dependent RNA polymerase (Elfiky, 2020), showed no antiviral effect (**Supplementary Table S3**). Favipiravir, approved by the National Medical Products Administration of China as the first anti-COVID-19 drug in China (Tu et al., 2020), showed only partial inhibitory activity at the non-toxic concentration of 100 µM (**Supplementary Table S3**).

We also assessed clinically approved protease inhibitors with potent activity against HIV-1. However, none of the HIV-1 protease inhibitors detailed in **Supplementary Table S3** showed remarkable protective antiviral activity against SARS-CoV-2 infection on Vero E6 cells, with the exception of nelfinavir mesylate hydrate, which showed an IC_{50} value below 10 µM (**Supplementary Table S3** and **Figure 2C**). Lopinavir and tipranavir inhibited SARS-CoV-2-induced cytopathic effect at the non-toxic concentration of 20 µM, and amprenavir exhibited activity at the non-toxic concentration of 100 µM (**Figure 2C**). Darunavir, which has been tested in clinical trials, showed partial inhibitory activity at 100 µM, although this concentration had 8.5 ± 6.2% of cytotoxicity associated (**Figure 2C**). Of note, we tested HIV-1 reverse transcriptase inhibitors such as tenofovir disoproxil fumarate, emtricitabin, tenofovir alafenamide, and their combinations, but they also failed to show any antiviral effect against SARS-CoV-2 (**Supplementary Table S1**). These results indicate that future clinical trials should contemplate the limited antiviral effect displayed by these anti-HIV-1 inhibitors against SARS-CoV-2 *in vitro*.

We also assessed the inhibitory capacity of HCV inhibitors, but none showed any antiviral activity (**Supplementary Table S3**). Of note, exogenous interferon-2α and interferon-γ displayed antiviral activity against SARS-CoV-2 (**Supplementary Table S3**). In light of these results, we tested the inhibitory effect of the TLR 7 agonist vesatolimod that triggers interferon

TABLE 1 | Compounds with antiviral activity ordered depending on their IC_{50} values on Vero E6. Notice that plitidepsin and cathepsin inhibitors display IC_{50} values in the nM range, while the rest of the compounds are in the µM or 10^2 IU/ml range.

	Drug	IC_{50}/CC_{50} µM (Mean +/− SD)	Mode of action	Previous clinical use	Vendor Origin
nM	Plitidepsin	0.06 +/− 0.02/> 0.1	Targets eukaryotic Elongation Factor 1A2 (eEF1A2)	Multiple myeloma	PharmaMar
	MDL 28170	0.14 +/− 0.06/> 87	Calpain III and Cathepsin B inhibitor	Pre-clinical	Merck
	NPO-2142; -2143 and -2260	~0.54/>10	Calpain and Cathepsin Inhibitors	Pre-clinical	Landsteiner Genmed
	Remdesivir	2.16 +/− 4.1/> 85	RNA Polymerase inhibitor	Ebola virus	Cayman Chemical
	Hydroxycloroquine	10.9 +/− 11.3/> 96	Clathrin-mediated endocitosys or pH-dependent viral fusion inhibitor	Malaria	Laboratories Rubio
<25 µM or 10^2IU/mL	Nelfinavir mesylate hydrate	Not calculated, but active < 10/ > 25	Protease inhibitor	HIV-1	Sigma Aldrich
	Chloroquine	3.86/>25	Clathrin-mediated endocitosys or pH-dependent viral fusion inhibitor	Malaria	Sigma Aldrich
	Interferon-2α	8.1+/−0.7 × 10^2 IU/mL/> 100 × 10^2 IU/mL	IFN stimulated antivirus proteins	Hepatitis and HIV-1	Sigma Aldrich
	interferon-γ	11.2 × 10^2 IU/mL/> 100 × 10^2 IU/mL	IFN stimulated antivirus proteins	Granulomatous disease	Sigma Aldrich
	Fenofibrate	19.8 +/− 8/>100	Activates PPARα	Dyslipidemia	Lacer

production. Although this agonist was not able to protect from the viral-induced cytopathic effect on Vero E6 (**Supplementary Table S3**), as expected since it is an interferon-producer deficient cell line (Emeny and Morgan, 1979), it could still be useful in other competent cellular targets. Since severe COVID-19 patients display impaired interferon responses (Hadjadj et al., 2020), these strategies may be valuable to avoid disease complication. In addition, we also assessed several compounds with the best computational docking scores among approved drugs against the 3CL protease of SARS-CoV-2, but none of them were effective to protect Vero E6 from viral induced cytopathic effect (**Supplementary Table S4**).

The most potent antiviral tested was plitidepsin (**Figure 2D**), which targets the eukaryotic Elongation Factor 1A2 (eEF1A2) and has been previously used for the treatment of multiple myeloma. The mean IC_{50} value of this drug in repeated experiments was always in nM concentrations (**Supplementary Table S3**). In combination with other active antivirals, we did not observe a reduction on IC_{50} values (**Supplementary Table S2**). This result indicates no significant synergy, but also highlights the possibility of using plitidepsin without reducing its antiviral activity in combined therapies (**Figure 2D**), what could be relevant to avoid possible selection of resistant viruses. Overall, plitidepsin showed the lowest IC_{50} values of all the compounds tested in this *in vitro* screening (**Table 1**).
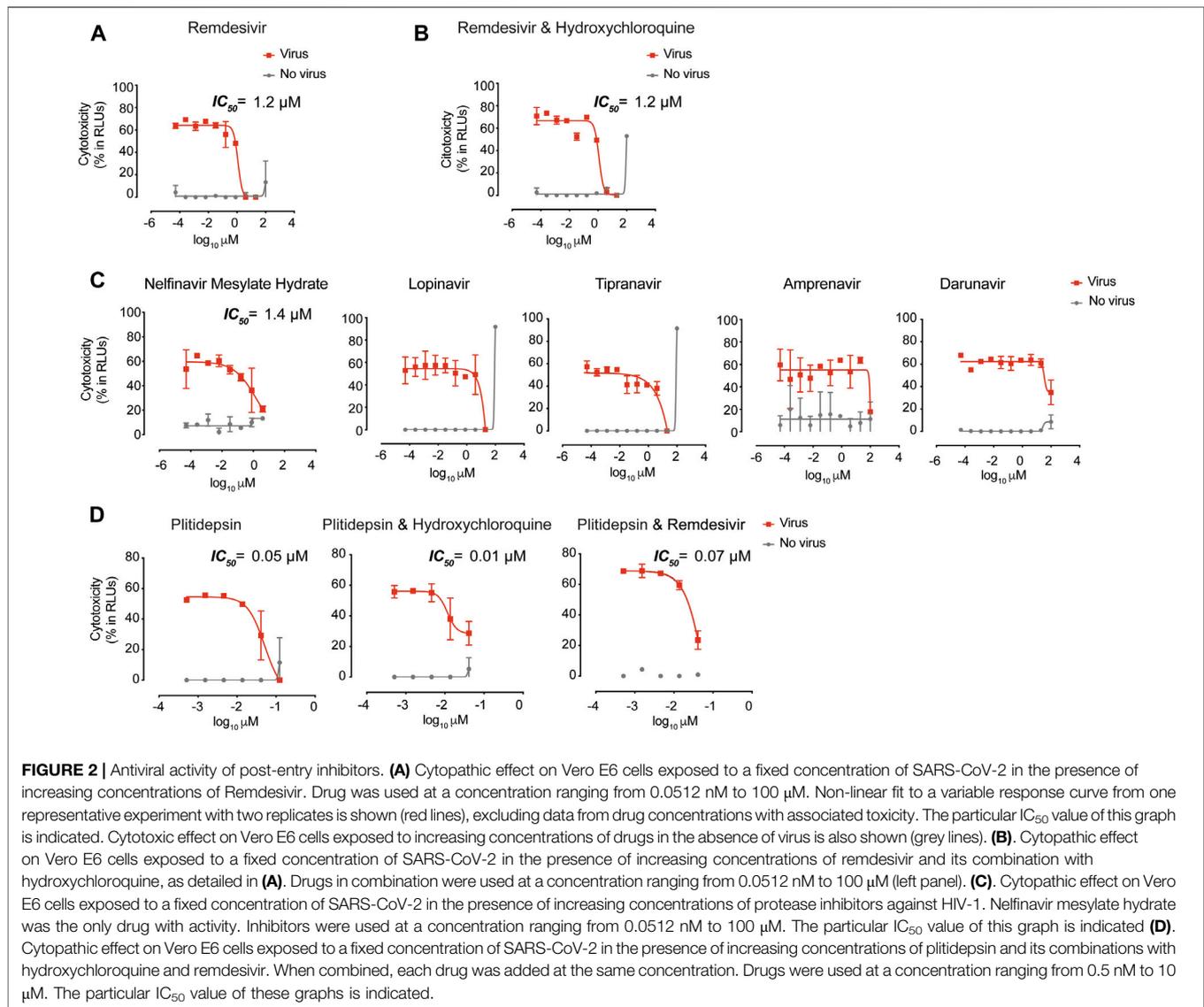
Antiviral Activity of Compounds with Unknown Mechanism of Action

We also assessed the inhibitory capacity of several inhibitors and broad anti-bacterial, anti-parasitic, anti-malarial, anti-influenza and anti-fungal compounds, along with other pharmacological agents previously suggested to interfere with SARS-CoV-2

infection (**Supplementary Table S5**). Such was the case of ivermectin, an FDA-approved broad spectrum anti-parasitic agent previously reported to inhibit the replication of SARS-CoV-2 *in vitro* as measured by RNA accumulation (Caly et al., 2020).

However, among these potential antivirals, only three types of molecules exerted detectable antiviral activity in our assay: itraconazole, fenofibrate, and calpain and cathepsin inhibitors such as MDL 28170 and NPO compounds. Itraconazole, an antifungal that may interfere with internal SARS-CoV-2 budding within infected cells (Wu et al., 2020), displayed an IC_{50} value of 80 µM (**Figure 3A** and **Supplementary Table S5**). Fenofibrate is clinically used to treat dyslipidemia via activation of PPARα, and also inhibited the cytopathic effect exerted by SARS-CoV-2 on Vero E6 at 20 µM (**Figure 3B** and **Supplementary Table S5**). As fenofibrate is a regulator of cellular lipid metabolism, we made use of the luciferase-based viral entry assay to try to elucidate its mode of action. When lentiviruses pseudotyped with the spike protein of SARS-CoV-2 were added to ACE2-expressing HEK-293 T cells in the presence of fenofibrate, viral entry was abrogated (**Figure 3C**). The most potent agent found was MDL 28170, a calpain III inhibitor in a pre-clinical stage of development that displayed activity in the nanomolar range (**Figure 3D** and **Supplementary Table S5**), as previously identified *in vitro* (Riva et al., 2020). Moreover, three out of four different calpain and cathepsin inhibitors named NPO showed potent antiviral activity too (**Supplementary Figure S2**). Of note, in combination with other active antivirals, we did not observe a reduction on IC_{50} values of MDL 28170 (**Supplementary Table S2**).

Inhibitors of calpains, which are cysteine proteases, might impair the activity of viral proteases like 3CL (main protease) and PLpro (papain-like protease) (Schneider et al., 2012; Riva et al., 2020). However, calpain inhibitors may also inhibit

FIGURE 2 | Antiviral activity of post-entry inhibitors. **(A)** Cytopathic effect on Vero E6 cells exposed to a fixed concentration of SARS-CoV-2 in the presence of increasing concentrations of Remdesivir. Drug was used at a concentration ranging from 0.0512 nM to 100 μM. Non-linear fit to a variable response curve from one representative experiment with two replicates is shown (red lines), excluding data from drug concentrations with associated toxicity. The particular IC$_{50}$ value of this graph is indicated. Cytotoxic effect on Vero E6 cells exposed to increasing concentrations of drugs in the absence of virus is also shown (grey lines). **(B)**. Cytopathic effect on Vero E6 cells exposed to a fixed concentration of SARS-CoV-2 in the presence of increasing concentrations of remdesivir and its combination with hydroxychloroquine, as detailed in **(A)**. Drugs in combination were used at a concentration ranging from 0.0512 nM to 100 μM (left panel). **(C)**. Cytopathic effect on Vero E6 cells exposed to a fixed concentration of SARS-CoV-2 in the presence of increasing concentrations of protease inhibitors against HIV-1. Nelfinavir mesylate hydrate was the only drug with activity. Inhibitors were used at a concentration ranging from 0.0512 nM to 100 μM. The particular IC$_{50}$ value of this graph is indicated **(D)**. Cytopathic effect on Vero E6 cells exposed to a fixed concentration of SARS-CoV-2 in the presence of increasing concentrations of plitidepsin and its combinations with hydroxychloroquine and remdesivir. When combined, each drug was added at the same concentration. Drugs were used at a concentration ranging from 0.5 nM to 10 μM. The particular IC$_{50}$ value of these graphs is indicated.

cathepsin B-mediated processing of viral spike proteins or glycoproteins, including SARS-CoV and Ebola (Schneider et al., 2012; Zhou and Simmons, 2012). To understand the mechanisms of action of calpain and cathepsin inhibitors such as MDL 28170, we added lentiviruses pseudotyped with the spike protein of SARS-CoV-2 to ACE2-expressing HEK-293T cells and the same cells also expressing TMPRSS2 in the presence of this drug. Importantly, MDL 28170 only blocked viral entry in ACE2-expressing cells (**Figure 3E**). This result indicates that MDL 28170 blocks cathepsins that are implicated in SARS-CoV-2 entry via the alternative endosomal pathway, as described for chloroquine derivatives and E-64d (**Figure 3E**), which are all active when TMPRSS2 is not present and their inhibitor camostat displays no activity (**Figure 3E**).

In conclusion, among the 72 compounds and their 28 combinations tested herein for their potential capacity to abrogate SARS-CoV-2 cytopathic effect, we only found 13 compounds with antiviral activity including camostat, and only eight types of these drugs had an IC$_{50}$ below 25 μM or 10^2 IU/ml (**Table 1**). These eight families of compounds were able to abrogate SARS-CoV-2 release to the supernatant in a dose dependent manner (**Figure 4**), indicating that the reduction in the cytopathic effect that we had measured in cells correlates with viral production. In the case of fenofibrate, however, this compound was less active inhibiting viral release as compared to the rest of the inhibitors tested (**Figure 4**), while still preserved cells from viral induced -cytopathic effect. As the eight families of compounds found tackle different steps of the viral life cycle, they could be tested in combined therapies to abrogate the potential emergence of resistant viruses.

FIGURE 3 | Antiviral activity of inhibitors with unknown mechanism of action. **(A)**. Cytopathic effect on Vero E6 cells exposed to a fixed concentration of SARS-CoV-2 in the presence of increasing concentrations of Itraconazole. Drug was used at a concentration ranging from 0.0512 nM to 100 μ. Non-linear fit to a variable response curve from one representative experiment with two replicates is shown (red lines), excluding data from drug concentrations with associated toxicity. The particular IC_{50} value of this graph is indicated. Cytotoxic effect on Vero E6 cells exposed to increasing concentrations of drugs in the absence of virus is also shown (grey lines). **(B)**. Cytopathic effect on Vero E6 cells exposed to a fixed concentration of SARS-CoV-2 in the presence of increasing concentrations of Fenofibrate, as detailed in **(A)**. **(C)**. Effect of fenofibrate on the entry of luciferase expressing lentiviruses pseudotyped with SARS-CoV-2 Spike in ACE2-expressing HEK-293T cells. Values are normalized to luciferase expression by mock-treated cells set at 100%. Mean and s.e.m. from two experiments with two replicates. Statistical deviations from 100% were assessed with a one sample t test. **(D)**. Cytopathic effect on Vero E6 cells exposed to a fixed concentration of SARS-CoV-2 in the presence of increasing concentrations of MDL 28170, as detailed in **(A)**. **(E)**. Comparison of MDL 28170 activity with entry inhibitors blocking viral endocytosis, such as chloroquine and E-64d, and inhibitors blocking serine protease TMPRSS2, such as camostat. ACE2 expressing HEK-293T cells transfected or not with TMPRSS2 were exposed to SARS-CoV-2 Spike lentiviruses in the presence of these compounds. Values are normalized to luciferase expression by mock-treated cells set at 100%. Mean and s.e.m. from at least two experiments with two replicates. Statistical deviations from 100% were assessed with a one sample t test.

FIGURE 4 | Decreased release of SARS-CoV-2 in the presence of inhibitors with antiviral activity. **(A)**. Viral release to the supernatant in the presence of the indicated compounds added at increasing concentrations 3 days post-infection of Vero E6 cells. SARS-CoV-2 nucleoprotein was detected with an ELISA at concentrations were drugs were nontoxic. Mean and s.e.m. from two experiments. **(B)**. Viral release to the supernatant in the presence of the indicated interferons as described in A. Mean and s.e.m. from one experiment.

DISCUSSION

We have assessed the anti-SARS-CoV-2 activity of clinically approved compounds that may exert antiviral effect alone or in combination. Although we were not able to detect any remarkable synergy *in vitro*, further work in more physiological cellular models is needed to address if any synergism and additivity can be found between identified compounds. Combined therapies are key to tackle viral infections and to reduce the appearance of viral resistance, and that is why identifying synergism and antagonism for SARS-CoV-2 antivirals is of key importance (Bobrowski et al., 2020). We have tested more than seventy compounds and their combinations, and verified a potent antiviral effect of hydroxychloroquine and remdesivir, along with plitidepsin, cathepsin and calpain inhibitors MDL 28170 and NPO, nelfinavir mesylate hydrate, interferon-2α, interferon-γ and fenofibrate. These are therefore the most promising agents found herein that were able to protect cells from viral-induced cytopathic effect by preventing viral replication.

Our findings highlight the utility of using hydroxychloroquine and MDL 28170 or other cathepsin inhibitors to block viral entry via the endosomal pathway in kidney cell lines such as Vero E6 or HEK-293T. However, the endosomal viral entry route is absent in pulmonary cells (Maisonnasse et al., 2020) and, therefore, camostat should be considered as the primary inhibitor to limit SARS-CoV-2 entry in pulmonary tissues or in cells expressing TMPRSS2 (Hoffmann et al., 2020). These findings can explain why randomized clinical trials using hydroxychloroquine have failed to show a significant protective effect (Boulware et al., 2020; Cavalcanti et al., 2020). Nonetheless, in combined therapies, it should be noted that agents targeting the alternative endosomal SARS-CoV-2 entry route such as hydroxychloroquine or MDL 28170 could be key to stop viral dissemination in other extrapulmonary tissues where viral replication has been already detected (Hanley et al., 2020), and viral entry could take place through this endosomal pathway. This could partially explain why in a retrospective observational study including more than 2500 patients, hydroxychloroquine treatment showed a significant reduction of in-hospital mortality (Arshad et al., 2020). Thus, since alternative routes govern SARS-CoV-2 viral entry depending on the cellular target (Ou et al., 2020a), effective treatments might be needed to block both plasma membrane fusion and endosomal entry to broadly achieve viral suppression.

SARS-CoV-2 replication could be effectively blocked using nelfinavir mesylate hydrate, remdesivir and plitidepsin. While nelfinavir showed lower potency, remdesivir and plitidepsin were the most potent agents identified. However, remdesivir and plitidepsin are not yet suitable for oral delivery and require intravenous injection, complicating their clinical use for prophylaxis. Finally, we also confirmed the antiviral effect of type I and II interferons as well as fenofibrate, which have been extensively used in the clinic for many years and may therefore prove valuable for therapeutic use.

The data presented herein should be interpreted with caution, as the IC_{50} values of drugs obtained *in vitro* may not reflect what could happen *in vivo* upon SARS-CoV-2 infection. The best antiviral compounds found in the present study need to be tested in adequate animal models. This strategy already helped to confirm the activity of remdesivir against SARS-CoV-2 (Williamson et al., 2020), while also questioning the use of hydroxychloroquine in monotherapy (Maisonnasse et al., 2020). Thus, assessing antiviral activity and safety in animal models is key to identify and advance those compounds with the highest potential to succeed in upcoming clinical trials. In turn, *in vitro* results confirmed in animal models will provide a rational basis to perform future clinical trials not only for treatment of SARS-CoV-2-infected individuals, but also for pre-exposure prophylaxis strategies that could avoid novel infections. Prophylaxis could be envisioned at a population level or to protect the most vulnerable groups, and should be implemented until an effective vaccine is developed. In particular, orally available compounds with proven safety profiles, such as fenofibrate, could represent promising agents.

DATA AVAILABILITY STATEMENT

The datasets presented in this study can be found in online repositories. The names of the repository/repositories and accession number(s) can be found below:
http://gisaid.org, EPI_ISL_510689.

ETHICS STATEMENT

The institutional review board on biomedical research from Hospital Germans Trias i Pujol (HUGTiP) approved this study. The individual who provided the sample to isolate virus gave a written informed consent to participate.

AUTHOR CONTRIBUTIONS

FUNDING

ACKNOWLEDGMENTS

We are grateful to patients at the Hospital Germans Trias i Pujol that donated their samples for research. For his excellent assistance and advice, we thank Jordi Puig from Fundació Lluita contra la SIDA. We are most grateful to Lidia Ruiz and the Clinical Sample Management Team of IrsiCaixa for their outstanding sample processing and management, and to M. Pilar Armengol and the translational genomics platform team at the Institut de Recerca Germans Trias i Pujol. We truly thank B. Trinité for generating the Spike expression plasmid construct used in this study. We thank Pharma Mar, Rubió Laboratories, Janssen and Drs. Cabrera and Ballana form IrsiCaixa; Pascual-Figal, Lax and Asensio-Lopez MC from "Instituto de Investigación Biosanitaria IMIB-Arrixaca" of Murcia; and Fernández-Real and Barretina from the "Institut d'Investigació Biomèdica de Girona Dr Josep Trueta" for providing some of the reagents tested.

SUPPLEMENTARY MATERIAL

The Supplementary Material for this article can be found online at: https://www.frontiersin.org/articles/10.3389/fphar.2021.646676/full#supplementary-material.

REFERENCES

Arshad, S., Kilgore, P., Chaudhry, Z. S., Jacobsen, G., Wang, D. D., Huitsing, K., et al. (2020). Treatment with hydroxychloroquine, azithromycin, and combination in patients hospitalized with COVID-19. *Int. J. Infect. Dis.* 97, 396–403. doi:10.1016/j.ijid.2020.06.099

Beigel, J. H., Tomashek, K. M., Dodd, L. E., Mehta, A. K., Zingman, B. S., Kalil, A. C., et al. (2020). Remdesivir for the treatment of covid-19-final report. *N. Engl. J. Med.* 383, 1813–1826. doi:10.1056/NEJMoa2007764

Bobrowski, T., Chen, L., Eastman, R. T., Itkin, Z., Shinn, P., Chen, C., et al. (2020). Discovery of synergistic and antagonistic drug combinations against SARS-CoV-2 in vitro. *BioRxiv.* doi:10.1101/2020.06.29.178889

Boulware, D. R., Pullen, M. F., Bangdiwala, A. S., Pastick, K. A., Lofgren, S. M., Okafor, E. C., et al. (2020). A randomized trial of hydroxychloroquine as postexposure prophylaxis for covid-19. *N. Engl. J. Med.*, 383, 517, doi:10.1056/NEJMoa2016638

Caly, L., Druce, J. D., Catton, M. G., Jans, D. A., and Wagstaff, K. M. (2020). The FDA-approved Drug Ivermectin inhibits the replication of SARS-CoV-2 *in vitro*. *Antiviral Res.* 178, 104787. doi:10.1016/j.antiviral.2020.104787

Cavalcanti, A. B., Zampieri, F. G., Rosa, R. G., Azevedo, L. C. P., Veiga, V. C., Avezum, A., et al. (2020). Hydroxychloroquine with or without azithromycin in mild-to-moderate covid-19. *N. Engl. J. Med.* 383, 2041–2052. doi:10.1056/NEJMoa2019014

Chen, C. Z., Shinn, P., Itkin, Z., Eastman, R. T., Bostwick, R., Rasmussen, L., et al. (2020a). Drug repurposing screen for compounds inhibiting the cytopathic effect of SARS-CoV-2. *BioRxiv.* doi:10.1101/2020.08.18.255877

Chen, N., Zhou, M., Dong, X., Qu, J., Gong, F., Han, Y., et al. (2020b). Epidemiological and clinical characteristics of 99 cases of 2019 novel coronavirus pneumonia in Wuhan, China: a descriptive study. *Lancet* 395, 507–513. doi:10.1016/S0140-6736(20)30211-7

Corman, V. M., Landt, O., Kaiser, M., Molenkamp, R., Meijer, A., Chu, D. K., et al. (2020). Detection of 2019 novel coronavirus (2019-nCoV) by real-time RT-PCR. *Euro. surveill* 25, 2000045. doi:10.2807/1560-7917.ES.2020.25.3.2000045

Dittmar, M., Lee, J. S., Whig, K., Segrist, E., Li, M., Jurado, K., et al. (2020). Drug repurposing screens reveal FDA approved drugs active against SARS-Cov-2. *bioRxiv.* doi:10.06.19.16104210.1101/2020.06.19.161042

Elfiky, A. A. (2020). Ribavirin, remdesivir, sofosbuvir, galidesivir, and tenofovir against SARS-CoV-2 RNA dependent RNA polymerase (RdRp): a molecular docking study. *Life Sci.* 253, 117592. doi:10.1016/j.lfs.2020.117592

Emeny, J. M., and Morgan, M. J. (1979). Regulation of the interferon system: Evidence that Vero cells have a genetic defect in interferon production. *J. Gen. Virol.* 43, 247–252. doi:10.1099/0022-1317-43-1-247

Fantini, J., Di Scala, C., Chahinian, H., and Yahi, N. (2020). Structural and molecular modelling studies reveal a new mechanism of action of chloroquine and hydroxychloroquine against SARS-CoV-2 infection. *Int. J. Antimicrob. Agents* 55, 105960. doi:10.1016/j.ijantimicag.2020.105960

Gassen, N. C., Papies, J., Bajaj, T., Dethloff, F., Emanuel, J., Weckmann, K., et al. (2020). Analysis of SARS-CoV-2-controlled autophagy reveals spermidine, MK-2206, and niclosamide as putative antiviral therapeutics. *BioRxiv.* doi:10.1101/2020.04.15.997254

Gautret, P., Lagier, J.-C., Parola, P., Hoang, V. T., Meddeb, L., Mailhe, M., et al. (2020). Hydroxychloroquine and azithromycin as a treatment of COVID-19: results of an open-label non-randomized clinical trial. *Int. J. Antimicrob. Agents* 56, 105949. doi:10.1016/j.ijantimicag.2020.105949

Gielen, V., Johnston, S. L., and Edwards, M. R. (2010). Azithromycin induces anti-viral responses in bronchial epithelial cells. *Eur. Respir. J.* 36, 646–654. doi:10.1183/09031936.00095809

Grein, J., Ohmagari, N., Shin, D., Diaz, G., Asperges, E., Castagna, A., et al. (2020). Compassionate use of remdesivir for patients with severe covid-19. *N. Engl. J. Med.*, 382, 2327. doi:10.1056/NEJMoa2007016

Gupta, A., and Zhou, H.-X. (2020). Profiling SARS-CoV-2 main protease (MPRO) binding to repurposed drugs using molecular dynamics simulations in classical and neural network-trained force fields. *ACS Comb. Sci.* 22, 826–832. doi:10.1021/acscombsci.0c00140

Hadjadj, J., Yatim, N., Barnabei, L., Corneau, A., Boussier, J., Smith, N., et al. (2020). Impaired type I interferon activity and inflammatory responses in severe COVID-19 patients. *Science*, 369, 718. doi:10.1126/science.abc6027

Hanley, B., Naresh, K. N., Roufosse, C., Nicholson, A. G., Weir, J., Cooke, G. S., et al. (2020). Histopathological findings and viral tropism in United Kingdom patients with severe fatal COVID-19: a post-mortem study. *Lancet Microb.* 1, E245–E253. doi:10.1016/S2666-5247(20)30115-4

Haviernik, J., Štefánik, M., Fojtíková, M., Kali, S., Tordo, N., Rudolf, I., et al. (2018). Arbidol (umifenovir): a broad-spectrum antiviral drug that inhibits medically important arthropod-borne flaviviruses. *Viruses* 10, 184. doi:10.3390/v10040184

Hoffmann, M., Kleine-Weber, H., Krüger, N., Müller, M., Drosten, C., and Pöhlmann, S. (2020). The novel coronavirus 2019 (2019-nCoV) uses the SARS-coronavirus receptor ACE2 and the cellular protease TMPRSS2 for entry into target cells. *Cell* 181, 271–280.e8. doi:10.1101/2020.01.31.929042

Ianevski, A., Yao, R., Fenstad, M. H., Biza, S., Zusinaite, E., Reisberg, T., et al. (2020). Potential antiviral options against SARS-CoV-2 infection. *Viruses* 12, 642. doi:10.3390/v12060642

Jeon, S., Ko, M., Lee, J., Choi, I., Byun, S. Y., Park, S., et al. (2020). Identification of antiviral drug candidates against SARS-CoV-2 from FDA-approved drugs. *Antimicrob. Agents Chemother.* 64.(7), e00819–e00820. doi:10.1128/aac.00819-20

Langmead, B., and Salzberg, S. L. (2012). Fast gapped-read alignment with Bowtie 2. *Nat. Methods* 9, 357–359. doi:10.1038/nmeth.1923

Li, H., Handsaker, B., Wysoker, A., Fennell, T., Ruan, J., Homer, N., et al. (2009). The sequence alignment/map format and SAMtools. *Bioinformatics* 25, 2078–2079. doi:10.1093/bioinformatics/btp352

Liu, J., Cao, R., Xu, M., Wang, X., Zhang, H., Hu, H., et al. (2020). Hydroxychloroquine, a less toxic derivative of chloroquine, is effective in inhibiting SARS-CoV-2 infection *in vitro*. *Cell Discov.* 6, 16. doi:10.1038/s41421-020-0156-0

Lu, Y., Liu, D. X., and Tam, J. P. (2008). Lipid rafts are involved in SARS-CoV entry into vero E6 cells. *Biochem. Biophysical. Res. Commun.* 369, 344–349. doi:10.1016/j.bbrc.2008.02.023

Maisonnasse, P., Guedj, J., Contreras, V., Behillil, S., Solas, C., Marlin, R., et al. (2020). Hydroxychloroquine use against SARS-CoV-2 infection in non-human primates. *Nature* 585 (7826), 584–587. doi:10.1038/s41586-020-2558-4

Martin, M. (2011). Cutadapt removes adapter sequences from high-throughput sequencing reads. *EMBnet. J.* 17, 310. doi:10.14806/ej.17.1.200

Mingo, R. M., Simmons, J. A., Shoemaker, C. J., Nelson, E. A., Schornberg, K. L., D'Souza, R. S., et al. (2015). Ebola virus and severe acute respiratory syndrome coronavirus display late cell entry kinetics: evidence that transport to NPC1+Endolysosomes is a rate-defining step. *J. Virol.* 89, 2931–2943. doi:10.1128/JVI.03398-14

Monteil, V., Kwon, H., Prado, P., Hagelkrüys, A., Wimmer, R. A., Stahl, M., et al. (2020) Inhibition of SARS-CoV-2 infections in engineered human tissues using clinical-grade soluble human ACE2. *Cell* 181(4):905–913. doi:10.1016/j.cell.2020.04.004

Münch, J. (2020). Alpha-1 antitrypsin inhibits SARS-CoV-2 infection. *BioRxiv* 14. doi:10.1101/2020.07.02.183764

Oguntuyo, K. Y., Stevens, C. S., Siddiquey, M. N., Schilke, R. M., Woolard, M. D., Zhang, H., et al. (2020). In plain sight: the role of alpha-1-antitrypsin in COVID-19 pathogenesis and therapeutics. *BioRxiv*. doi:10.1101/2020.08.14.248880

Ou, T., Mou, H., Zhang, L., Ojha, A., Choe, H., and Farzan, M. (2020a). Hydroxychloroquine-mediated inhibition of SARS-CoV-2 entry is attenuated by TMPRSS2. *Plos Pathog.* 17 (1), e1009212. doi:10.1371/journal.ppat.1009212

Ou, X., Liu, Y., Lei, X., Li, P., Mi, D., Ren, L., et al. (2020b). Characterization of spike glycoprotein of SARS-CoV-2 on virus entry and its immune cross-reactivity with SARS-CoV. *Nat. Commun.* 11, 1620. doi:10.1038/s41467-020-15562-9

Pan, H. (2020). Repurposed antiviral drugs for COVID-19–interim WHO Solidatary trial results. *BioRxiv* 17. doi:10.1101/2020.10.15.20209817

Richardson, P., Griffin, I., Tucker, C., Smith, D., Oechsle, O., Phelan, A., et al. (2020). Baricitinib as potential treatment for 2019-nCoV acute respiratory disease. *The Lancet* 395, e30–e31. doi:10.1016/S0140-6736(20)30304-4

Riva, L., Yuan, S., Yin, X., Martin-Sancho, L., Matsunaga, N., Pache, L., et al. (2020). Discovery of SARS-CoV-2 antiviral drugs through large-scale compound repurposing. *Nature* 586 (7827):113–119. doi:10.1038/s41586-020-2577-1

Schneider, M., Ackermann, K., Stuart, M., Wex, C., Protzer, U., Schätzl, H. M., et al. (2012). Severe acute respiratory syndrome coronavirus replication is severely impaired by MG132 due to proteasome-independent inhibition of M-calpain. *J. Virol.* 86, 10112–10122. doi:10.1128/JVI.01001-12

Simmons, G., Gosalia, D. N., Rennekamp, A. J., Reeves, J. D., Diamond, S. L., and Bates, P. (2005). Inhibitors of cathepsin L prevent severe acute respiratory syndrome coronavirus entry. *Proc. Natl. Acad. Sci.* 102, 11876–11881. doi:10.1073/pnas.0505577102

Song, Z., Xu, Y., Bao, L., Zhang, L., Yu, P., Qu, Y., et al. (2019). From SARS to MERS, thrusting coronaviruses into the spotlight. *Viruses* 11, 59. doi:10.3390/v11010059

Stebbing, J., Phelan, A., Griffin, I., Tucker, C., Oechsle, O., Smith, D., et al. (2020). COVID-19: combining antiviral and anti-inflammatory treatments. *Lancet Infect. Dis.* 20, 400–402. doi:10.1016/S1473-3099(20)30132-8

Tu, Y.-F., Chien, C.-S., Yarmishyn, A. A., Lin, Y.-Y., Luo, Y.-H., Lin, Y.-T., et al. (2020). A review of SARS-CoV-2 and the ongoing clinical trials. *Ijms* 21, 2657. doi:10.3390/ijms21072657

Wang, M., Cao, R., Zhang, L., Yang, X., Liu, J., Xu, M., et al. (2020). Remdesivir and chloroquine effectively inhibit the recently emerged novel coronavirus (2019-nCoV) *in vitro*. *Cell Res.* 30, 269–271. doi:10.1038/s41422-020-0282-0

Weston, S., Coleman, C. M., Haupt, R., Logue, J., Matthews, K., Li, Y., et al. (2020). Broad anti-coronavirus activity of Food and drug administration-approved drugs against SARS-CoV-2 *in vitro* and SARS-CoV *in vivo*. *J. Virol.* 94. e01218–20. doi:10.10.1128/jvi.01218-20

WHO (2020). "Solidarity" clinical trial for COVID-19 treatments. Available at: https://www.who.int/emergencies/diseases/novel-coronavirus-2019/global-research-on-novel-coronavirus-2019-ncov/solidarity-clinical-trial-for-covid-19-treatments (Accessed August 18, 2020).

Williamson, B. N., Feldmann, F., Schwarz, B., Meade-White, K., Porter, D. P., Schulz, J., et al. (2020). Clinical benefit of remdesivir in rhesus macaques infected with SARS-CoV-2. *Nature* 585 (7824), 273–276. doi:10.1038/s41586-020-2423-5

Wu, C., Liu, Y., Yang, Y., Zhang, P., Zhong, W., Wang, Y., et al. (2020). Analysis of therapeutic targets for SARS-CoV-2 and discovery of potential drugs by computational methods. *Acta Pharmaceutica. Sinica B* 10, 766–788. doi:10.1016/j.apsb.2020.02.008

Zhou, Y., and Simmons, G. (2012). Development of novel entry inhibitors targeting emerging viruses. *Expert Rev. Anti-infective Ther.* 10, 1129–1138. doi:10.1586/eri.12.104